Theor. Appl. Climatol. 86, 147–160 (2006)
DOI 10.1007/s00704-005-0217-1

Theoretical and Applied Climatology
Printed in Austria

[1] Global Change Impact Studies Centre/Pakistan Meteorological Department, Islamabad, Pakistan
[2] Abdus Salam International Centre for Theoretical Physics, Trieste, Italy

Effect of remote forcings on the winter precipitation of central southwest Asia part 1: observations

F. S. Syed[1], **F. Giorgi**[2], **J. S. Pal**[2], and **M. P. King**[2]

With 11 Figures

Received December 17, 2004; revised June 23, 2005; accepted September 1, 2005
Published online July 5, 2006

Summary

We investigate the effects of the North Atlantic Oscillation (NAO) and the El Nino Southern Oscillation (ENSO) on winter precipitation in Central Southwest Asia (CSWA) using an analysis of available observed climate data. The analysis is based on correlations, composites and Singular Value Decomposition (SVD) performed using the gridded dataset of the Climatic Research Unit (CRU) and station data for the region. We find that both the NAO and ENSO affect climate over the region. In particular a positive precipitation anomaly is typically found in correspondence of the positive NAO phase and warm ENSO phase over a sub-region encompassing northern Pakistan, Afghanistan, Tajikistan and southern Uzbekistan. This conclusion is supported by a consistency across the different analysis methods and observation datasets employed in our study. A physical mechanism for such effect is proposed, by which western disturbances are intensified over the region as they encounter a low pressure trough, which is a dominant feature during positive NAO and warm ENSO conditions. Our results give encouraging indications towards the development of statistically-based prediction tools for winter precipitation over the CSWA region.

1. Introduction

The Central Southwest Asia region (CSWA) includes Afghanistan, Iran, Western India, Tajikistan, Turkmenistan, Pakistan and Uzbekistan. This region has very complex topography (Fig. 1) and the orientation and height of the mountain ranges play an important role in determining precipitation. The main mountain ranges of the region include the western portion of the Himalayas (which extend from east to west up to the Karakoram Range in Pakistan), the Hindu Kush in Afghanistan, the Pamir Mountains in Tajikistan and the Zagros Mountain range in southwestern Iran.

The vegetation of CSWA ranges from steppe to desert and with large areas that receive little or no precipitation. The spatial distribution of winter precipitation (as defined by the period December–January–February–March or DJFM) is shown in Fig. 2a. In Iran, Afghanistan and Tajikistan, precipitation primarily falls in the winter, resulting from eastward-propagating mid-latitude cyclones from the Mediterranean region (Martyn, 1992). These systems are often observed as closed cyclonic circulations at sea-level and are usually called Western Disturbances (WDs) (Pisharoty and Desai, 1956). Most of the moisture forming precipitation is intercepted and condensed due to the presence of the high mountain ranges of the region, while the interior high plains are left with large stretches of barren desert. At the higher elevations, much of the precipitation falls as snow, and therefore the timing

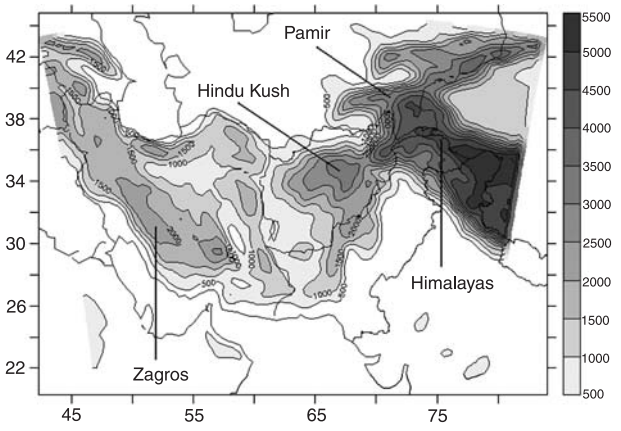

Fig. 1. Topography of the CSWA region (m)

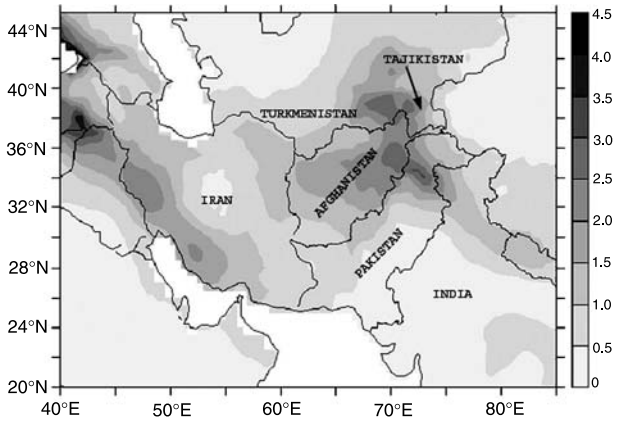

a)

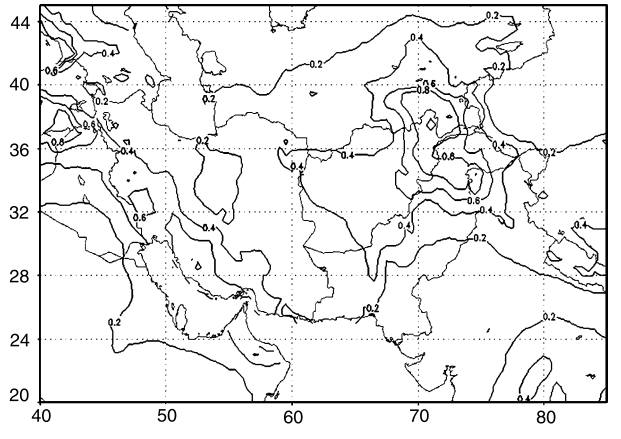

b)

Fig. 2. (**a**) Average DJMF precipitation (mm/day) over the CSWA region for the period 1950–2000. (**b**) Standard Deviation of seasonal DJFM precipitation (mm/day) for the period 1950–2000

and amount of snowmelt is an important factor for the water management and agriculture of the region. In eastern Pakistan and western India, the primary rainfall season is summer, and is induced by the north-western advance of the South Asia monsoon. However, winter precipitation in the form of snow still constitutes a primary water reserve for these areas and is responsible for the perennial flow of rivers throughout the year.

The Indian monsoon does not penetrate into Afghanistan, Iran and Tajikistan. With the exception of the irrigated Indus Valley of Pakistan, the cropland/pasture and forest areas of CSWA receive the largest amounts of winter rainfall. These areas include the western side of the Zagros mountains in western Iran, the northern side of the Albroz mountains in northern Iran, and the slopes of the Hindu Kush in Afghanistan (Agrawala et al., 2001).

The interannual variability of winter precipitation is relatively large in the CSWA region (Fig. 2b) and is characterized by episodes of severe droughts. For example, during the period 1998–2002, the CSWA experienced the most severe drought conditions in the last 50 years (Barlow et al., 2002). This drought has been linked to sea surface temperature (SST) anomalies in the tropical Pacific and Indian Oceans (Barlow et al., 2002; Hoerling and Kumar, 2003).

Many studies (Ropelewski and Halpert, 1996) have attempted to relate anomalous precipitation patterns across the globe to ENSO. In addition, NAO is a dominant mode of winter variability in the Northern Hemisphere, its effect extending from North America to Europe and a large portion of Asia (Hurrell et al., 2003). The positive NAO phase is related to stronger than average westerly winds across the mid latitudes of the Atlantic, an intensification and northward shift of the North Atlantic storm track and enhanced moisture-flux convergence from Iceland to Scandinavia (Hurrell, 1995; Rodwell et al., 1999; Cullen and deMenocal, 2000). During the negative NAO phase the north-Atlantic storm track is displaced southward, bringing relatively wet conditions over the Mediterranean and dry conditions over Northern Europe (Hurrell, 1995, 1996). The NAO exhibits multi-decadal trends, and a strong trend towards the positive phase has been observed in recent decades (Hurrell, 1995, 1996).

While a multitude of studies have investigated the effects of ENSO and the NAO on regional climates, little work has focused on the CSWA

region, particularly concerning winter precipitation which, as mentioned, is critical for the management of water resources there. As a limited example, a positive correlation between the NAO and precipitation over the western and northwestern regions of Iran was found by Jafar and Zeinolabedin (2003). In this paper, we thus present for the first time a comprehensive analysis of the effect of ENSO and the NAO on winter precipitation variability over the CSWA region.

Since winter precipitation over CSWA primarily comes from WDs traveling from the Mediterranean and Eastern Europe, it can be expected that the NAO might have an influence on CSWA winter precipitation. In addition, ENSO is a pervasive phenomenon that, through teleconnection patterns, affects climate not only in the tropical Pacific, but also in remote regions (Trenberth, 1998). The effects of the NAO and ENSO can also be significantly modulated by local forcings, for example due to topography (e.g. Cintia et al., 2003; Bojariu and Giorgi, 2005). Furthermore, the frequency and characteristics of the NAO and ENSO are likely to be modified by the effect of increases in anthropogenic greenhouse gases and atmospheric aerosols (Cubasch et al., 2001). It is thus important from the perspective of water resources prediction and management to better understand the influence of remote forcings on precipitation in CSWA and the key processes underlying this influence.

In this paper, we study the effects of the NAO and ENSO on the CSWA winter precipitation via an analysis of available observations and reanalysis data over the region. This analysis makes use of correlations, composites and SVD (see Sect. 2). In future work, we plan to investigate the underlying physical mechanisms using a series of regional climate model simulations. It is important to emphasize that a better understanding of the influence of ENSO and the NAO on CSWA winter precipitation might provide important insights into the predictability of this precipitation and might thus help in the design of suitable prediction tools.

2. Data and methods

In this study, the NAO is measured by the winter (DJFM) NAO index (NAOI) of Hurrell (1995). The NAOI is based on the normalized sea level pressure (SLP) difference between Lisbon, Portugal and Stykkisholmur/Reykjavik, Iceland. The SLP anomalies at each station are normalized by dividing each seasonal mean pressure by the corresponding standard deviation calculated over the long term period (1864–1983) (see http://www.cgd.ucar.edu/cas/jhurrell/nao.stat.winter.html). The normalization is used to avoid the series being dominated by the greater variability of the northern station. In this study we consider the period from 1951 to 2000 (see below).

The Southern Oscillation Index (SOI) is one measure of the large-scale fluctuations in air pressure between the western and eastern tropical Pacific (i.e. the state of the Southern Oscillation) during El Niño and La Niña episodes. Traditionally, this index is calculated from the pressure anomaly difference between Tahiti and Darwin, Australia. In general, smoothed time series of the SOI are very consistent with changes in ocean temperature across the eastern tropical Pacific. The negative phase of the SOI represents below-normal air pressure at Tahiti and above-normal air pressure at Darwin. Prolonged periods of negative SOI values coincide with abnormally warm ocean waters across the eastern tropical Pacific (El Niño episode or warm ENSO phase) while prolonged periods of positive SOI values coincide with abnormally cold ocean waters across the eastern tropical Pacific (La Niña episode or cold ENSO phase).

The large scale circulation data (SLP, 500 hPa and 200 hPa geopotential heights) used in our analysis are from the National Center for Environmental Prediction/National Center for Atmospheric Research (NCEP/NCAR) reanalysis (Kalnay et al., 1996). For Meteorological observations over land, we use the Climate Research Unit, CRU TS 2.0 dataset (Mitchell et al., 2003), which includes monthly surface air temperature and precipitation for the period 1901–2000 on a regular global 0.5 degree land surface grid. This dataset revises and extends the original dataset of New et al. (2000). It should be noted that in areas with sparse station coverage, such as CSWA, the CRU dataset interpolates grid point values from the nearest available stations. This may thus add a significant element of uncertainty. We focus on the period 1951–2000 because of the availability of both the NCEP-NCAR data and CRU observa-

tions in this period. For this period we also have available data from 26 meteorological stations distributed throughout Pakistan and obtained from the Central Data Processing Centre, Pakistan Meteorological Department, Karachi, Pakistan. We find generally good consistency between these station data and the CRU data.

2.1 Analysis methods

In our analysis we first use composites and correlation patterns between the NAOI or the SOI and precipitation. A year is considered to be in a positive (negative) NAO phase when the NAOI is more than one standard deviation above (below) the average NAOI for 1951–2000. An analogous definition is applied to positive and negative SOI years. The composites are calculated as the difference between the ensemble average of positive NAOI (or SOI) years and that of negative NAOI (or SOI) years. During the 1951–2000 period we found 10 positive NAOI years (1973, 1981, 1983, 1989, 1990, 1992, 1993, 1994, 1995, 2000), 9 negative NAOI years (1955, 1962, 1963, 1964, 1965, 1969, 1977, 1979, 1996), 7 positive SOI years (1956, 1971, 1974, 1976, 1989, 1999, 2000) and 7 negative SOI years (1978, 1983, 1987, 1990, 1992, 1993, 1998). Therefore, some years can be positive (or negative) for both the NAOI and the SOI. Standard Pearson's correlation coefficients r are calculated in the correlation analysis, and a two tailed t-test is used to assess the significance of the Pearson's r.

Some stations over Pakistan show high interannual variability with instances of DJFM precipitation values close to zero. Visual inspection of precipitation PDFs at individual stations indicated that a Gamma Distribution is best suited to calculate the standard deviation for the station data as a measure of interannual variability. Sen and Eljadid (1999) also found that gamma distribution is the probability distribution of monthly rainfall in arid regions. The probability density function of a Gamma Distribution is as follows:

$$g(x) = \frac{1}{\beta^{\alpha}\Gamma(\alpha)} x^{\alpha-1} e^{-x/\beta}$$

where $\alpha > 0$ is the shape parameter, $\beta > 0$ is the scale parameter, $x > 0$ is the precipitation amount and $\Gamma(\alpha)$ is the gamma function. The maximum likelihood estimates of α and β are calculated. The mean and Variance are then calculated as

$$E(x) = \alpha\beta \qquad \mathrm{Var}(x) = \alpha\beta^2$$

The standard deviation is then given by the square root of the variance.

We also use Singular Value Decomposition (SVD) analysis. Some examples of the use of this technique may be found in Uvo and Berndtsson (1996), Wallace et al. (1992, 1993), and Uvo et al. (1998). Newman and Sardeshmukh (1995) discuss the issues related to SVD analysis used to recover the relationship between two fields. Note that this analysis is commonly used in studies of coupled climate signals and therefore only its salient features are described here. The reader is referred to Bretherton et al. (1992) for the basic theory and mathematical steps required to carry out SVD analysis. The SVD analysis had been found to give robust results compared with other methods for extracting coupled signals, it has a small systematic bias and is relatively easy to implement, and therefore it has been recommended for general use (Bretherton et al., 1992).

The SVD of the cross-covariance matrix between sea level pressure and precipitation generates pairs of spatial patterns that maximize the temporal covariance between the two fields and a vector of singular values. A homogeneous map of a field for a particular mode is the vector of correlations between the time series of grid-point values of that field and the time series of expansion coefficients for that mode of the same field. A heterogeneous correlation map of a field for a particular mode is the vector of correlations between the time series of the grid points values of that field and the time series of the expansion coefficients for that mode of another field. In this paper, attention is given to the heterogeneous correlation maps over the CSWA region as we seek the influence of SLP on CSWA precipitation. The correlation coefficients between the time series of the expansion coefficients for the leading mode of the two fields are also calculated.

The squared covariance fraction (SCF) for a particular mode is the ratio of the squared singular value for that mode and the sum of the squared singular values for all modes (as computed by Bretherton et al., 1992). The SCF is therefore an indication of the proportion of covariance explained by a particular mode.

3. Results and discussion

3.1 North Atlantic oscillation

3.1.1 Composite and correlation analysis

Figure 3a shows the composite (positive minus negative NAO phase) of winter (DJFM) precipitation over the CSWA region. This shows an area of maximum positive composite precipitation of 0.4 to 1.0 mm/day extending from the Hindu Kush mountain range in Afghanistan to northern Pakistan and adjacent areas of northern India. These values can be compared with an average precipitation of 2–4 mm/day over this region. A positive precipitation composite is also observed in northern and northwestern Iran, which is consistent with the findings of Jafar and Zeinolabedin (2003). The westernmost areas of CSWA, including the eastern Mediterranean region and central and southern Iran, show negative composite values. Other small areas of negative precipitation composites are found close to the northern borders of Pakistan and Afghanistan.

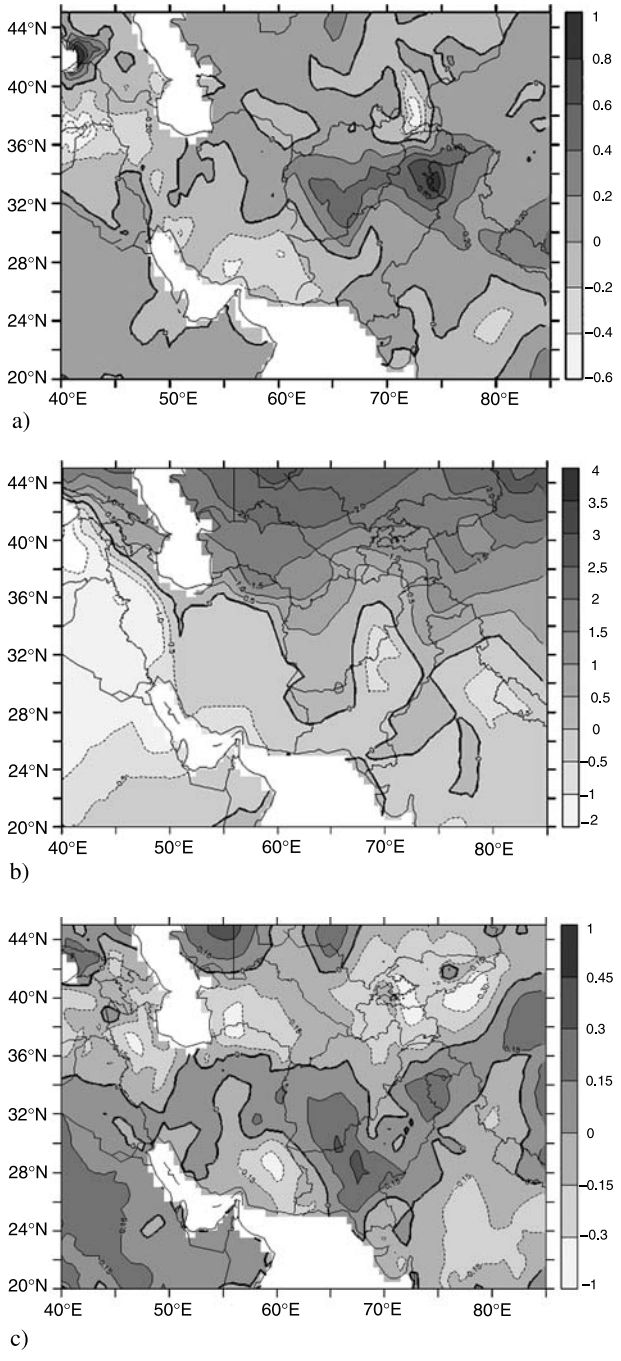

Fig. 3. (**a**) NAO composite of precipitation (mm/day). (**b**) NAO composite of surface temperature (°C). (**c**) Correlation Coefficient between the NAOI and CSWA precipitation

The temperature composites (Fig. 3b) show positive values over the northern regions of CSWA and negative values extending from the eastern Mediterranean to central Iran and southern Pakistan. The correlation between the NAOI and CSWA winter precipitation (Fig. 3c) shows features mostly in agreement with the composite map (Fig. 3a). The highest positive correlations are found over northern Pakistan and southeastern Afghanistan. This latter maximum extends to southern Pakistan, although the composite does not show a strong signal there because southern Pakistan receives low precipitation amounts during the winter.

In agreement with the precipitation composites, negative correlations are found over the eastern Mediterranean, southern Iran, and northern CSWA (Turkmenistan, Uzbekistan and Tajikistan). We also find that the composites and correlations match well with those derived from the Pakistan station data (see Table 1 and the discussion in Sect. 3.3). Note that the dry conditions during the positive NAO phase over the Mediterranean region do not correspond to dry conditions over most of the CSWA region.

A number of studies have shown a weakening and decreasing number of cyclones over the Mediterranean area during the rainy season (October through March) in the last decades, (Maheras et al., 2000, 2001; Trigo et al., 2000). This tendency is strongest in the western Mediterranean and weakens towards the central Mediterranean, where the frequency of cyclones has not shown a substantial decrease. In fact, an anal-

Table 1. List of Meteorological Stations of Pakistan along with Latitude, Longitude, Elevation, Mean (1951–2000) DJFM precipitation, Standard Deviation of DJFM precipitation (1951–2000), NAOI and SOI Correlation with winter CSWA precipitation and CSWA precipitation composites. The stations are arranged in descending order with respect to Latitude

Station	Lat. (N)	Long. (E)	Elev. (m)	Ave. (mm/day)	S.D.	NAO		SOI	
						Corr.	Comp. (mm/day)	Corr.	Comp. (mm/day)
Gilgit	35° 55′	74° 20′	1460	0.23	0.15	−0.12	−0.04	−0.04	−0.05
Drosh	35° 34′	71° 47′	1465	2.37	0.83	+0.02	0.45	−0.27*	0.46
Astore	35° 22′	74° 54′	2168	1.69	0.66	+0.15	0.39	−0.28*	0.33
Skardu	35° 18′	75° 41′	2210	0.87	0.61	+0.22	0.34	−0.15	0.26
Muzaffarabad	34° 22′	73° 29′	702	3.98	1.40	+0.25	1.16	−0.23	1.46
Garhi Dupatta	34° 13′	73° 37′	813	4.41	1.49	−0.05	−0.10	−0.37**	1.99
Kakul	34° 11′	73° 15′	1309	3.14	0.91	+0.18	0.55	−0.33*	1.17
Risalpur	34° 04′	71° 59′	315	1.70	0.76	+0.15	0.45	−0.38**	0.97
Peshawar	34° 01′	71° 35′	360	1.45	0.69	+0.19	0.43	−0.45**	1.12
Murree	33° 55′	73° 23′	2168	4.09	1.97	+0.42**	2.12	−0.35**	2.42
Parachinar	33° 52′	70° 05′	1729	2.65	1.15	+0.01	0.02	−0.13	0.83
Islamabad	33° 37′	73° 06′	508	2.13	0.80	+0.24	0.62	−0.28*	0.58
Kotli	33° 31′	73° 54′	615	2.87	1.18	+0.33*	1.19	−0.28*	1.11
Jhelum	32° 56′	73° 43′	234	1.58	0.85	+0.29*	0.69	−0.31*	1.19
D. I. Khan	31° 49′	70° 55′	174	0.65	0.33	+0.15	0.19	−0.27*	0.32
Lahore	31° 31′	74° 24′	216	0.85	0.51	+0.42**	0.38	−0.33*	0.63
Faisalabad	31° 26′	73° 06′	184	0.51	0.36	+0.08	0.03	−0.09	0.27
Zhob	31° 21′	69° 28′	1407	0.89	0.44	+0.09	0.10	+0.03	−0.11
Quetta	30° 15′	66° 53′	1601	1.53	0.79	+0.27*	0.53	−0.12	0.63
Bahawalpur	29° 24′	71° 47′	117	0.26	0.21	−0.06	−0.01	−0.21	0.14
Kalat	29° 02′	66° 35′	2017	1.05	0.95	–	0.30	–	1.29
Dalbaden	28° 53′	64° 24′	850	0.54	0.36	−0.04	−0.06	−0.04	0.16
Panjgur	26° 58′	64° 06′	981	0.51	0.35	−0.16	−0.16	−0.04	0.10
Hyderabad	25° 23′	68° 25′	41	0.09	0.08	+0.18	0.03	+0.07	−0.05
Pasni	25° 16′	63° 29′	6	0.70	0.65	−0.11	−0.05	+0.02	0.10
Karachi	24° 54′	67° 08′	22	0.28	0.32	+0.06	0.15	+0.07	−0.01

* Significant at 95% confidence level
** Significant at 99% confidence level

ysis of the Atlas of Extratropical Storm Tracks produced by NASA (http://www.giss.nasa.gov/data/stormtracks/) indicates that the frequency and direction of WDs, which usually originate from the central and eastern Mediterranean, do not appear to be significantly affected by the NAO (analysis not shown).

The NAO composites of SLP and 500 hPa heights (Fig. 4) show a prominent trough over the CSWA region. This trough appears to be an eastward and southeastward extension of the Icelandic low. Decades of a predominantly strong Siberian anticyclone from the 1950s to the 1970s were followed by a period (essentially since the 1980s) with significantly weakened high pressure and a distinct temperature rise in this area (Sahsamanoglou et al., 1991). In particular, Hurrell and Van Loon (1997) and Thompson et al. (2000a) show that the positive phase of the NAO yields enhanced advection of warm air over extra-tropical Eurasia north of about 45° N. The positive phase of the NAO is thus likely an important cause of the winter half-year warming in Siberia and northern Europe (Hurrell, 1996). In our composite analysis, we also find a ridge in the surface temperature patterns (Fig. 3b) in correspondence of the SLP trough over the CSWA region. This is induced by the advection of relatively warm air from central and northern Europe during the positive NAO phase.

3.1.2 Singular Value Decomposition (SVD) analysis

We computed a SVD of the temporal cross-covariance matrix between SLP in the north

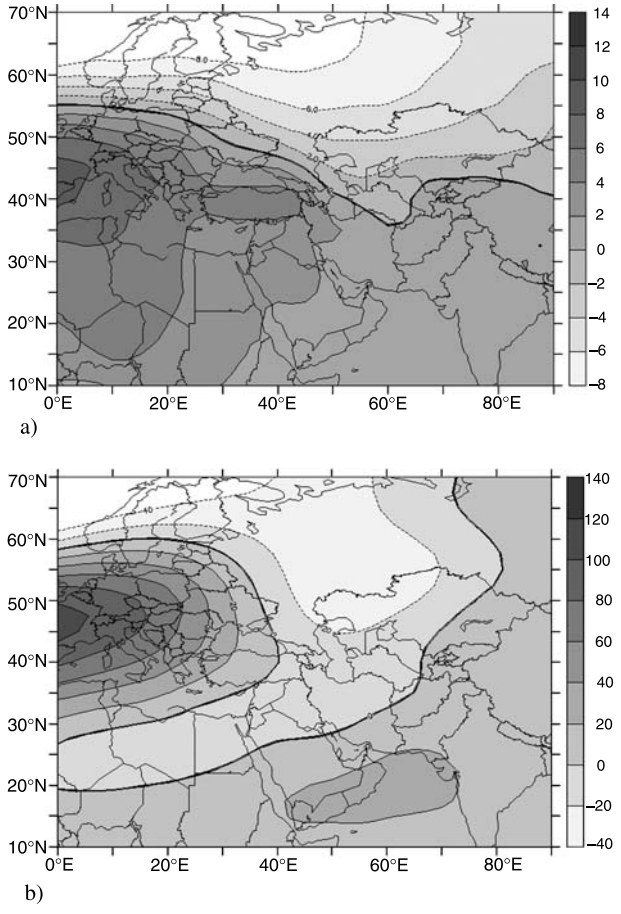

Fig. 4. (**a**) NAO composite of SLP (hPa). (**b**) NAO composite of 500 hPa heights (m)

Atlantic (the domain in Fig. 5a) and precipitation in CSWA (the domain in Fig. 5b). We find SCF values of up to 60% for the north Atlantic SLP and CSWA precipitation leading mode. Figure 5a, b are the heterogeneous correlation maps for north Atlantic SLP and CSWA precipitation. This shows patterns similar to the correlation maps between the NAOI and CSWA precipitation (see Fig. 3c). The expansion coefficient time series (ECS1) for the leading mode of north Atlantic SLP has a correlation of 0.86 with the NAOI (Fig. 5c). The SVD analysis thus confirms the results discussed in Sect. 3.1 and provides added objective information that the NAO is the leading variability mode over the north Atlantic and is responsible for the precipitation pattern seen in the composite and correlation analysis over the CSWA region.

3.2 El Nino Southern oscillation forcing

3.2.1 Composite and correlation analysis

Results from the composite and correlation analysis applied to the ENSO forcing of CSWA winter precipitation are presented in Fig. 6a, c. The composite analysis shows a positive maximum of 0.4 to 1.0 mm/day along the Himalayas and Karakoram Range in northern Pakistan and the Pamir Mountains in Tajikistan, which can be compared to an average precipitation of 2–4 mm/day over this region (1951–2000). Positive composite precipitation values are also found over most of Iran (especially the southern coastal areas) and the central regions of Afghanistan and Pakistan. Small areas of negative composite precipitation occur over southern Iran and northern Afghanistan. The correlation patterns (Fig. 6c) are generally consistent with the composite precipitation patterns, with the highest correlations occurring over northern Pakistan and the Pamir region. Both the composites and correlations match well with the Pakistan station data of Table 1 (discussed in Sect. 3.3).

The temperature composite map shows warm conditions over western Russia and Siberia in correspondence of the warm ENSO phase. In addition, a tongue of warm air extends from northern Afghanistan to southern Iran and Pakistan in the CSWA region. These results are consistent with those of Hurrell (1996).

The composites of SLP and 500 hPa heights (Fig. 7) show a trough extending over the CSWA region as a result of an ENSO teleconnection. Although the structure of the ENSO-related trough is similar to that of the NAO-related trough over the CSWA area, the underlying process appears different. While the NAO-related trough is associated with an eastward extension of the Icelandic low, the ENSO-related trough appears to occur in conjunction with a weaker than normal establishment of the Siberian High. In addition, the ENSO-related trough has a more pronounced north-south orientation than the NAO-related one, which extends more in an east-west direction.

3.2.2 Singular Value Decomposition (SVD) analysis

We computed SVD of the temporal cross-covariance matrix between SLP over the Wes-

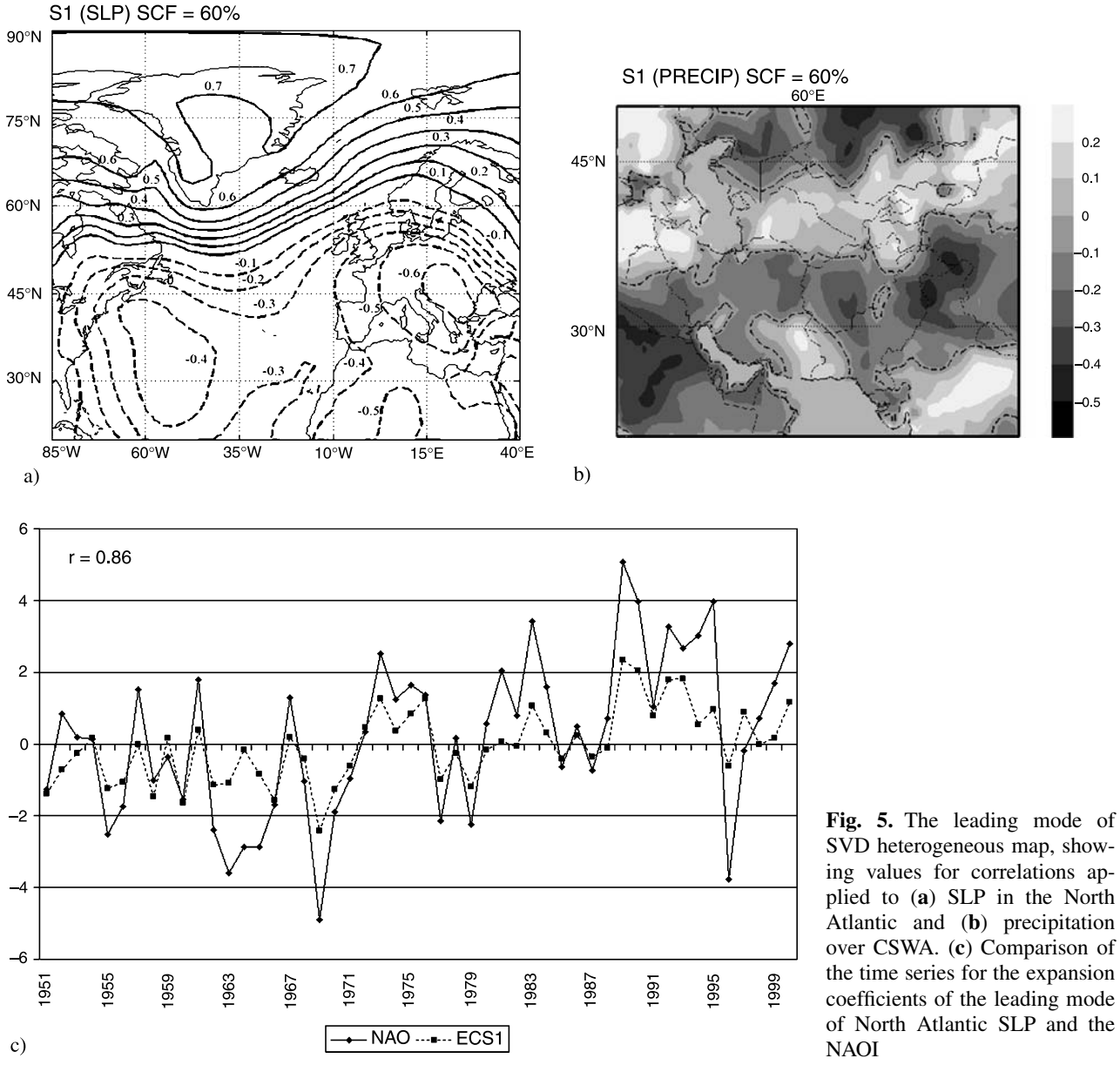

Fig. 5. The leading mode of SVD heterogeneous map, showing values for correlations applied to (**a**) SLP in the North Atlantic and (**b**) precipitation over CSWA. (**c**) Comparison of the time series for the expansion coefficients of the leading mode of North Atlantic SLP and the NAOI

tern Pacific (domain in Fig. 8a) and CSWA precipitation. We find SCF values of 62% for the leading modes of western Pacific SLP and CSWA precipitation. Figure 8a, b show the heterogeneous correlation maps for these leading modes, which shows patterns similar to the ones in the correlation map between SOI and CSWA precipitation (Fig. 6c). The leading mode expansion coefficient time series for the western Pacific SLP has a correlation of 0.94 with the SOI, indicating that the leading mode of variability over the western Pacific which has the highest covariability with the CSWA precipitation is ENSO. This again provides further supporting evidence of the effect of ENSO on CSWA precipitation.

3.3 More detailed analysis of NAO and ENSO effects on precipitation over Pakistan

In the previous sections we investigated the effects of the NAO and ENSO on CSWA winter precipitation by utilizing the CRU gridded observation dataset. As mentioned in Sect. 2, we also have available precipitation data from 26 stations throughout Pakistan covering the period 1951–2000. Because a spatial interpolation procedure is employed to calculate the CRU gridded

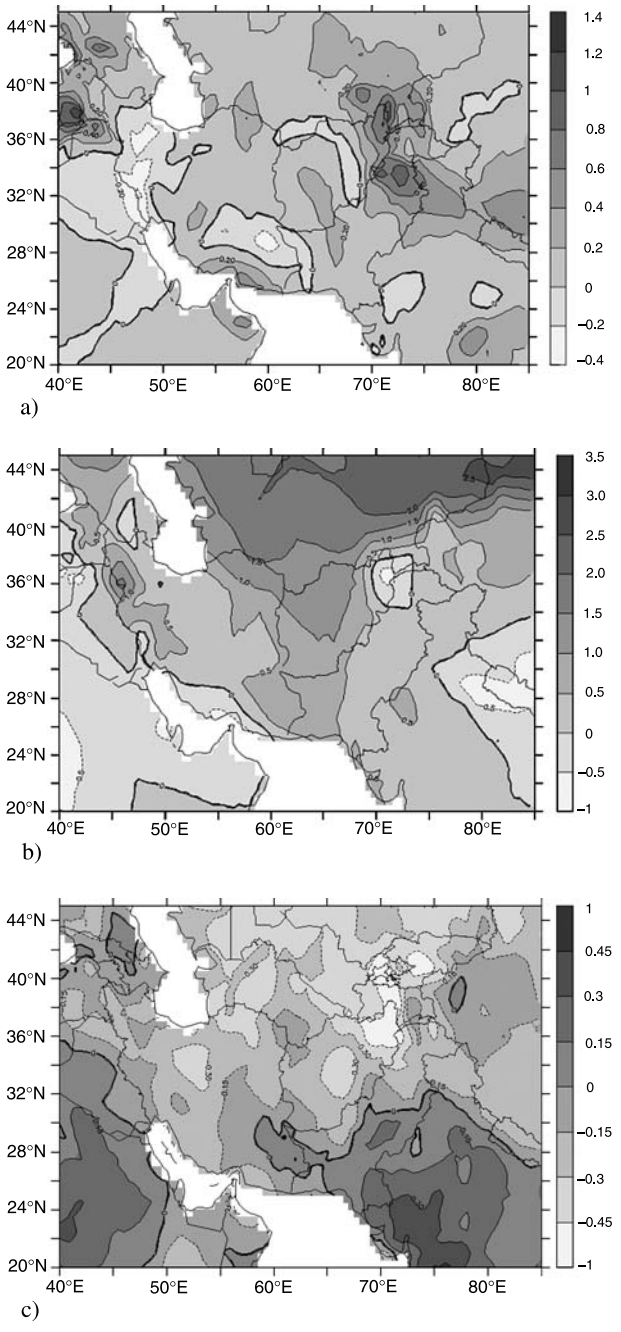

Fig. 6. (**a**) SOI composite of precipitation (mm/day). (**b**) SOI composite of surface temperature (°C). (**c**) Correlation coefficients between the SOI and CSWA precipitation

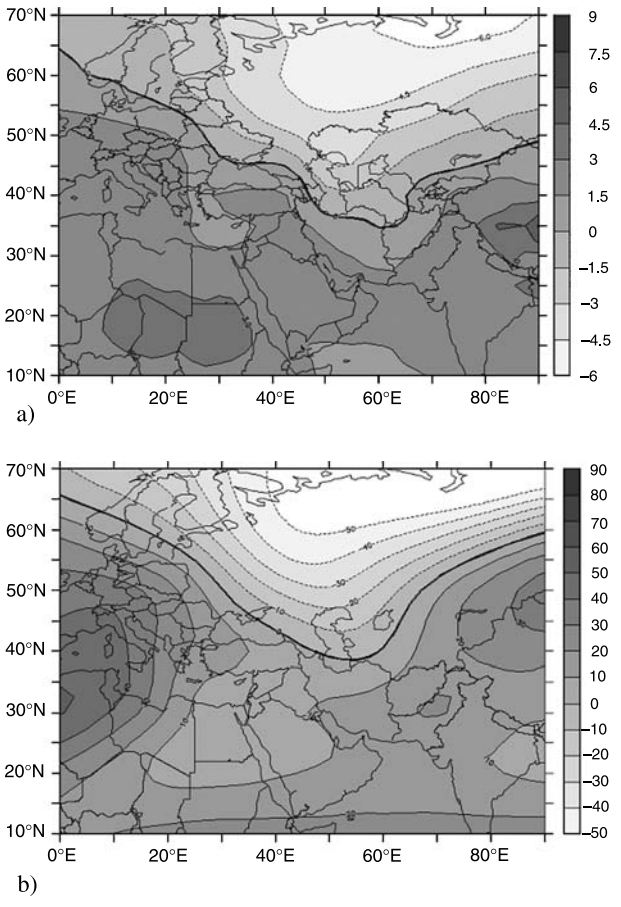

Fig. 7. (**a**) SOI composite of SLP (hPa). (**b**) SOI composite of 500 hPa heights (m)

data over station sparse regions (such as CSWA), it is useful to compare the results obtained with the CRU dataset with those obtained using the Pakistan station dataset.

Table 1 presents, for the period 1951–2000, the latitude, longitude, elevation, average DJFM precipitation, standard deviation of DJFM precipitation, and DJFM precipitation correlations and composites for the NAOI and SOI, respectively, for each of the 26 stations. The NAO is positively correlated with precipitation and shows a positive composite value over most stations. Exceptions to this feature occur mostly over stations that receive very low precipitation amounts. Similarly, the SOI (which is negative for the warm ENSO phase) is negatively correlated with precipitation and shows positive composite values at most stations. The stations in the north (Drosh, Astore, Skardu, Muzaffarabad, Garhi Dupatta, Kakul, Risalpur, Peshawar, Jhelum, Murree, Islamabad, Kotli, and D.I. Khan) and west (Quetta) of Pakistan, where average precipitation is more than 20 mm/month (0.7 mm/day), generally show higher values of correlation and composite. In addition, it appears that ENSO has a more significant effect on winter precipitation over Pakistan than the NAO, since more stations with statistically significant correlations are found for the SOI than the NAOI. Also note that

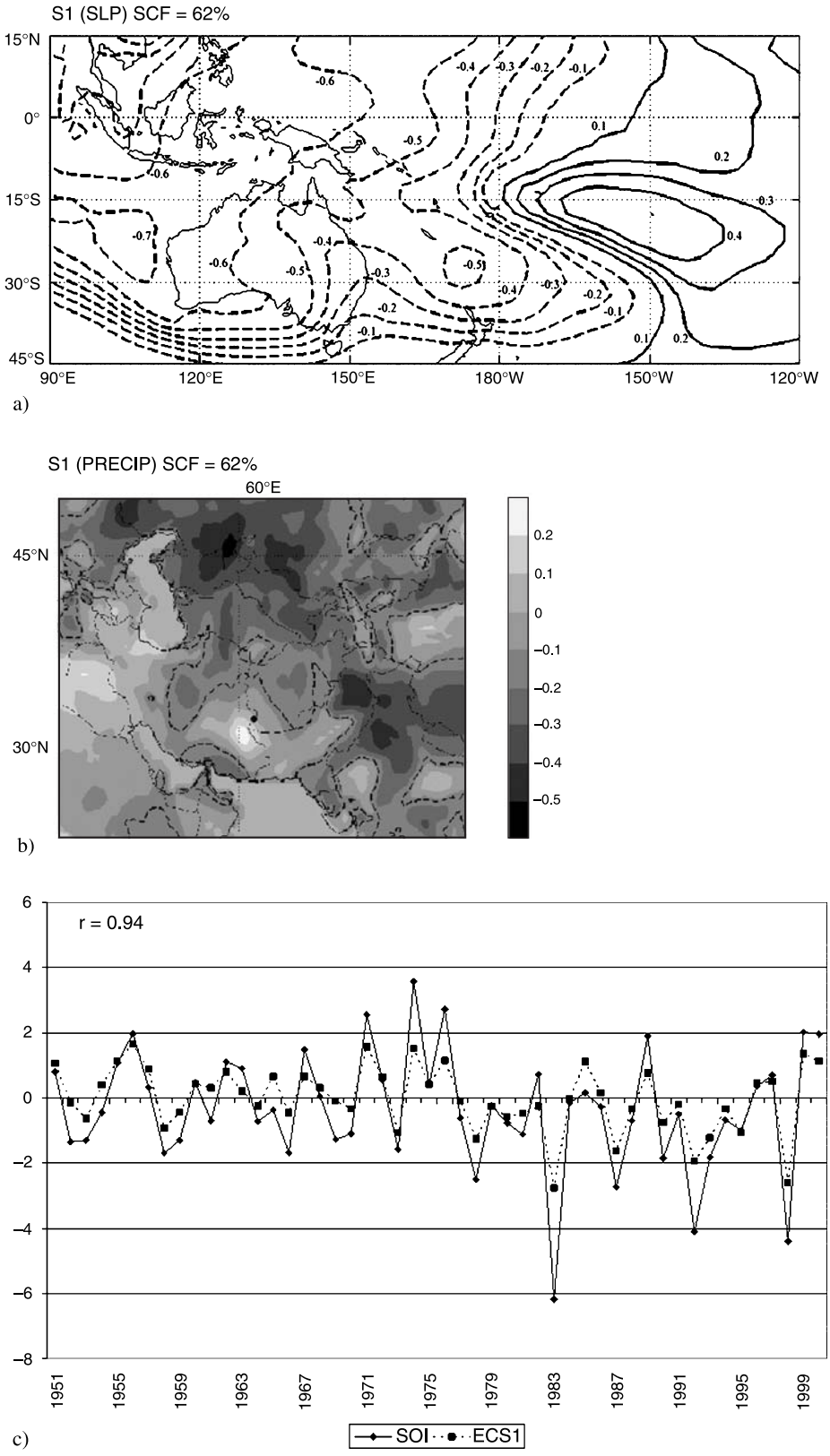

Fig. 8. The leading mode of SVD heterogeneous map, showing values for correlations applied to (**a**) SLP in the western Pacific and (**b**) precipitation over CSWA. (**c**) Comparison of the time series for the expansion coefficients of the leading mode of western Pacific SLP and the SOI

the ENSO composites are above one standard deviation at all stations where the SOI correlations are statistically significant.

Comparison of the correlations and composites in Table 1 with those reported in Figs. 3 and 6 show a high level of consistency

between the CRU-based and station-based results.

3.4 Combined effect of NAO and ENSO on the CSWA winter precipitation trends

In the previous sections we have seen how both the NAO and ENSO significantly affect the winter precipitation over the CSWA region. The main centers of action for the NAO and ENSO effects occur over the same area encompassing northern Pakistan, central and northern Afghanistan, Taijikistan and south-eastern Uzbekistan. It can thus be expected that long term trends in precipitation over this region are also affected by trends in the NAO and ENSO.

Figure 9 shows the time series of NAOI, and -1^{*}SOI along with their linear trends. In both cases we see an increasing trend, pronounced for the NAOI and relatively smaller for the SOI. The trend observed in recent decades towards an increasingly positive phase of the NAO is well documented in the literature, while more debate

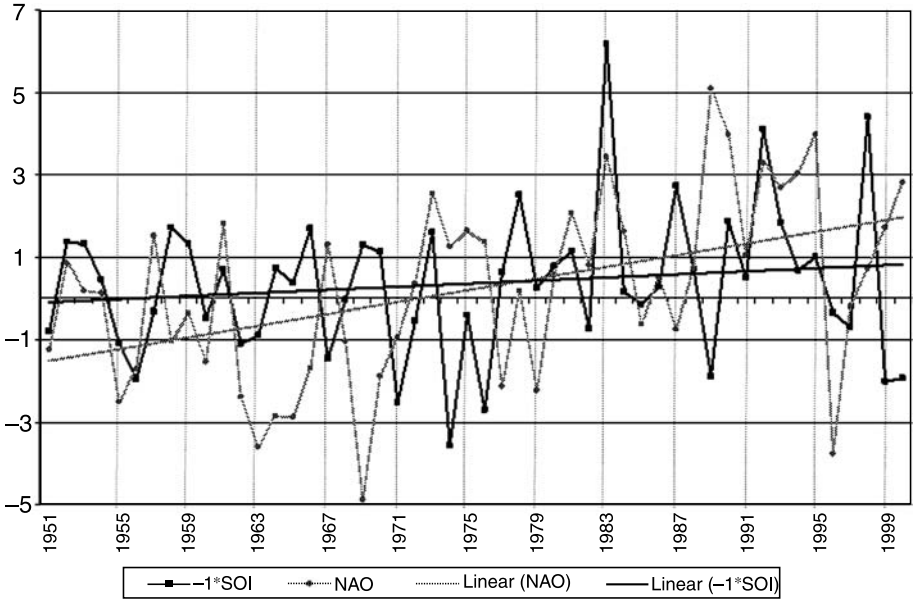

Fig. 9. Time series of NAOI and -1^{*} SOI and their respective linear trends from 1956 to 2000

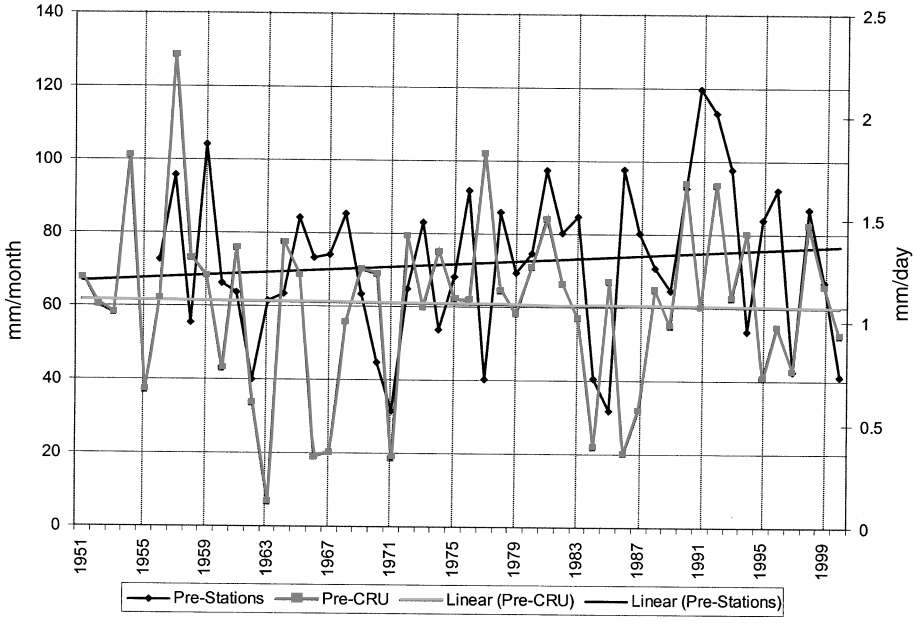

Fig. 10. Time series of average winter precipitation (mm/month) at 17 stations over Pakistan (see text) and CRU precipitation (mm/day) over the region (28°–40° N; 60°–80° E)

exists on trends in ENSO (Hurrell, 1995; Jacobeit et al., 2001).

Figure 10 shows time series and linear trends of precipitation calculated from two sources: the CRU data averaged over the region (28–40 N; 60–80 E) and the Pakistan stations where the average DJFM precipitation is greater than 20 mm/month or 0.7 mm/day (see Table 1), which comprises stations mostly located in northern Pakistan. In the case of the station, data we find a positive precipitation trend consistent with the trends in NAOI and SOI. When using the CRU data over the larger region the trend is small for the overall 1951–2000 period. If we, however, restrict our analysis to the period 1963–2000, when the largest increase in NAOI is found, then a positive precipitation trend becomes more evident also in the CRU dataset.

It is obviously difficult to unambiguously infer a cause-effect relationship from the SOI and NAOI trends of Fig. 9 and the precipitation trends of Fig. 10, and longer time series would be needed to more fully explore possible trend relationships. This is particularly so in view of the fact that both the SOI and NAOI show the same trend sign during the analysis period, so it is difficult to separate the effects of ENSO and NAO. However, the different sets of trends are at least qualitatively consistent with each other and therefore are suggestive of additional evidence of the influence of ENSO and NAO on the CSWA precipitation.

3.5 Proposed mechanism

A proposed physical mechanism to explain the effect of ENSO and the NAO on CSWA precipitation, and in particular the increase in CSWA precipitation during the positive phase of NAO and the warm phase of ENSO, is depicted in Fig. 11. As mentioned, WDs responsible for winter precipitation over CSWA originate from the Mediterranean. It is proposed that as the WDs move towards the east, they encounter a region of enhanced low pressure over Afghanistan and central Asia induced by the southward extent of the troughs identified in correspondence of the positive NAO and warm ENSO phases. As a result, the WDs gain strength over northern Iran and Afghanistan, possibly receiving additional moisture from the Caspian and Arabian Seas, and produce increased precipitation over Afghanistan, Tajikistan, northern Pakistan and southern Uzbekistan. The greater meridional orientation of the composite precipitation effect in the ENSO case compared to the NAO case is due to the deeper meridional extension of the ENSO-related trough.

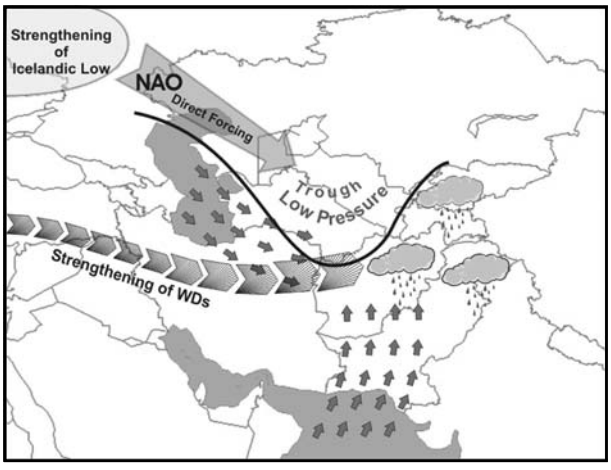

a)

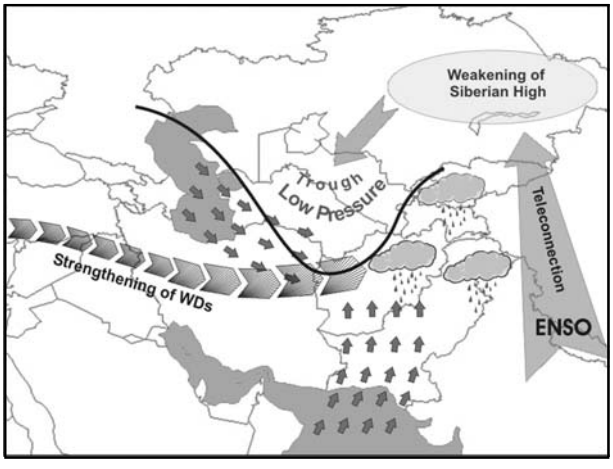

b)

Fig. 11. Proposed mechanism for the effect of (**a**) the positive NAO phase and (**b**) warm ENSO phase on winter precipitation over CSWA, respectively

4. Conclusions

In this work, we carry out an investigation of observed winter precipitation over the CSWA region using composites, correlation and SVD analysis. Our objective is to identify the possible influence of NAO and ENSO on winter precipitation over CSWA and study the spatial and temporal variability of this influence. The correlation

of CSWA precipitation with the NAOI and SOI, along with the consistency between the composites and the correlations, point towards a significant effect of both the NAO and ENSO on the observed winter precipitation in the CSWA region. This effect is especially evident over a subregion of CSWA encompassing northern Pakistan, Afghanistan, Tajikistan and southern Uzbekistan, where we observe a positive (negative) precipitation anomaly in correspondence of the positive (negative) NAO phase and the warm (cold) ENSO phase. We also find some consistency between recent multi-decadal trends in the NAO, ENSO and winter station precipitation over Pakistan.

In the positive NAO and warm ENSO phases, a trough develops over the mid CSWA region, although the origin and orientation of the trough are different between the ENSO and NAO cases. In the case of the NAO the trough results from an eastward extension of the Icelandic Low, and it is relatively shallow and zonally oriented. In the case of ENSO, the trough is associated with the establishment of a weak Siberian High and it is deeper and has a more meridional orientation. As a result, the NAO-related precipitation signal is mostly oriented in an east–west direction while the ENSO-related precipitation signal is more oriented in a north–south direction.

We propose a physical mechanism of the NAO and ENSO effects on winter CSWA precipitation by which WDs originating in the Mediterranean and crossing this region are intensified when they reach the low pressure trough and release precipitation as they hit the western slopes of the Himalaya, Karakoram and Pamir mountain ranges. We are currently performing regional climate model simulations to elucidate the physical processes underlying this proposed mechanism and for report in a future paper.

The substantial forcing of CSWA winter precipitation by both the NAO and ENSO provides encouraging indications towards the development of predictive tools for winter CSWA precipitation. It can be envisioned that indexes of circulation features associated with the NAO and ENSO could be used as statistical model predictors for CSWA precipitation. We are currently investigating the feasibility of constructing statistically-based prediction models of winter CSWA precipitation.

Acknowledgements

F. S. Syed thanks the Physics of Weather and Climate Section of the Abdus Salam International Centre for Theoretical Physics, Trieste, Italy, for inviting him as a visiting scientist to work on the subject of this paper. Discussions with Dr. Fred Kucharski were highly enlightening and much appreciated. Finally, we thank two anonymous reviewers for their careful reviews and very useful comments.

References

Agrawala S, Barlow M, Cullen H, Lyon B (2001) The drought and humanitarian crisis in central and southwest Asia: a climate perspective. IRI Report, IRI, Palisade, NY. Available at: http://iri.columbia.edu/outreach/publication/irireport/SWAsia/index.html [Accessed 15 July 2004]

Barlow M, Cullen H, Lyon B (2002) Drought in central and southwest Asia: La Nina, the warm pool, and Indian Ocean precipitation. J Clim 15: 697–700

Bojariu R, Giorgi F (2005) The north Atlantic oscillation signal in a regional climate simulation for the European region. Tellus A (in press)

Bretherton CS, Smith C, Wallace JM (1992) An intercomparison of methods for finding coupled patterns in climate data. J Clim 5(6): 541–560

Cintia B, Uvo C (2003) Analysis and regionalization of Northern European winter precipitation based on its relationship with the North Atlantic oscillation. Int J Climatol 23: 1185–1194

Cubasch U et al (2001) Projections of future climate change. In: Climate change 2001: The Scientific Basis. Cambridge: Cambridge University Press, pp 525–582

Cullen H, deMenocal PB (2000) North Atlantic influence on Tigris Euphrates stream flow. Int J Climatol 20: 853–863

Hoerling M, Kumar A (2003) The perfect ocean for drought. Science 299: 691–694

Hurrell JW, Kushnir Y, Visbeck M, Ottersen G (2003) An overview of the North Atlantic oscillation. The North Atlantic oscillation: Climate significance and environmental impact. AGU Geophysical Monograph Series, 134

Hurrell JW (1995) Decadal trends in the North Atlantic oscillation: regional temperature and precipitation. Science 269: 676–679

Hurrell JW (1996) Influence of variations in extratropical wintertime teleconnections on Northern Hemisphere temperature. Geophys Res Lett 23: 665–668

Hurrell JW, van Loon H (1997) Decadal variations in climate associated with the North Atlantic oscillation. Climatic Change 36: 301–326

Jacobeit J, Jonsson P, Barring L, Beck C, Ekstrom M (2001) Zonal indices for Europe (1780–1995) and running correlations with temperature. Climatic Change 48: 219–241

Jafar NM, Zeinolabedin S (2003) The influence of the North Atlantic oscillation on autumnal precipitation over Western and Northwestern parts of Iran. Book of Abstracts p 45, climate processes and climate change. RMS Conference UEA, Norwich

Kalnay E, Kanamitsu M, Kistler R, Collins W, Deaven D, Gandin L, Iredell M, Saha S, White G, Woollen J, Zhu Y, Chelliah M, Ebisuzaki W, Higgins W, Janowiak J, Mo KC, Ropelewski C, Wang J, Leetmaa A, Reynolds R, Jenne B, Joseph D (1996) The NCEP/NCAR 40-year reanalysis project. Bull Amer Meteor Soc 77(3): 437–472

Maheras P, Patrikas I, Karacostas Th, Anagnostopoulou Chr (2000) Automatic classification of circulation types in Greece: methodology, description, frequency, variability and trend analysis. Theor Appl Climatol 67: 205–223

Maheras P, Flocas HA, Patrikas I, Anagnostopoulou Chr (2001) A 40 year objective climatology of surface cyclones in the Mediterranean region: spatial and temporal distribution. Int J Climatol 21: 109–130

Martyn D (1992) Climates of the world. Elsevier first edition, 436 pp

Mitchell TD, Carter TR, Jones PD, Hulme M, New M (2003) A comprehensive set of high-resolution grids of monthly climate for Europe and the globe: the observed record (1901–2000) and 16 scenarios (2001–2100). J Climate (submitted)

New M, Hulme M, Jones P (2000) Representing twentieth century space-time climate variability. Part 2: development of 1901–96 monthly grids of terrestrial surface climate. J Climate 13: 2217–2238

Newman M, Sardeshmukh PD (1995) A caveat concerning singular value decomposition. J Climate 8: 352–360

Pisharoty PR, Desai BN (1956) Western disturbances and Indian weather. Indian J Meteorol 8: 333–338

Rodwell MJ, Rowell DP, Folland CK (1999) Oceanic forcing of the wintertime North Atlantic oscillation and European climate. Nature 398: 320–323

Ropelewski CF, Halpert MS (1996) Quantifying southern oscillation precipitation relationships. J Climate 9: 1043–1059

Sahsamanoglou H, Makrogiannis T, Kallimopoulos P (1991) Some aspects of the basic characteristics of the Siberian anticyclone. Int J Climatol 11: 827–839

Sen Z, Eljadid AG (1999) Rainfall distribution function for Libya and rainfall prediction. Hydrol Sci J 44(5): 665–680

Thompson LG, Yao T, Mosley-Thompson E, Davis ME, Henderson KA, Lin PN (2000) A high resolution millennial record of the South Asian Monsoon from Himalayan ice cores. Science 289: 1916–1919

Trenberth KE, Branstator GW, Karoly D, Kumar A, Lau N-C, Ropelewski C (1998) Progress during TOGA in understanding and modeling global teleconnections associated with tropical sea surface temperatures. J Geophys Res (special TOGA issue) 103: 14291–14324

Trigo IF, Davies TD (2000) Decline in Mediterranean rainfall caused by weakening of Mediterranean cyclones. Geophys Res Lett 27(28): 2913–2916

Uvo C, Berndtsson R (1996) Regionalization and special properties of Ceara state rainfall in northeast Brazil. J Geophys Res 101: 4221–4233

Uvo CRB, Repelli CA, Zebiak SE, Kushnir Y (1998) The relationship between tropical pacific and Atlantic SST and northeast Brazil monthly precipitation. J Climate 11: 551–562

Wallace JM, Smith C, Bretherton CS (1992) Singular value decomposition of wintertime sea surface temperature and 500-mb height anomalies. J Climate 5: 561–576

Wallace JM, Zang Y, Lau K-H (1993) Structure and seasonality of interannual and interdecadal variability of geopotential height and temperature fields in the Northern hemisphere troposphere. J Climate 6: 2063–2082

Authors' addresses: F. S. Syed, Global Change Impact Studies Centre/Pakistan Meteorological Department, Islamabad, Pakistan; F. Giorgi, J. S. Pal, M. P. King, Abdus Salam International Centre for Theoretical Physics, 34014, Trieste, Italy.